Proc. Annual Meeting of the Austrian Society for Biomedical Engineering 2021
DOI: 10.3217/978-3-85125-826-4-07

EFFECTS OF DISEASE PROGRESSION ON MECHANICAL STRESSES IN HUMAN ABDOMINAL AORTIC ANEURYSMS

E. Klimstein[1], M. Dalbosco[1], G.A. Holzapfel[1,2]

[1] Institute of Biomechanics, Graz University of Technology, Austria
[2] Department of Structural Engineering, NTNU, Norway

e.klimstein@student.tugraz.at, mdalbosco@tugraz.at, holzapfel@tugraz.at

Abstract — *The present study uses finite element (FE) simulations to investigate a three-stage theory on the pathogenesis of abdominal aortic aneurysms (AAAs). The effect of collagen growth and remodeling (G&R) on mechanical wall stresses during disease evolution is investigated. The results show that impaired remodeling during AAA growth leads to an increase in wall stress, indicating a more vulnerable vessel. Conversely, successful G&R of the collagen network results in less stress, suggesting a possible healing process promoted by vascular cells that sense the mechanical changes associated with AAA formation and growth. Overall, the results presented provide valuable insights into the pathogenesis of AAAs.*

Keywords — *Abdominal aortic aneurysm, finite element method, growth and remodeling*

Introduction

Abdominal aortic aneurysms (AAAs) are abnormal dilatations of the infrarenal aorta that are usually diagnosed when their diameter is greater than 30mm [1, 2]. If left untreated, AAAs can protrude to the point of rupture, an event that leads to death in up to 90% of cases [3, 4]. Elective surgery usually reduces the likelihood of rupture [1, 5]; however, the risk associated with the surgical procedure must also be considered. Even if other parameters such as growth rate or life expectancy are sometimes taken into account in this context [6], the decision for surgical intervention is usually made on the basis of the size of the AAA: patients are operated when the aneurysm diameter reaches 5.0cm (in females) or 5.5cm (in males) [6, 7].

However, reports of ruptured aneurysms smaller than these thresholds as well as stable larger aneurysms have raised questions about the suitability of this empirical standard [8]. Therefore, better criteria for aneurysm risk assessment are needed. To achieve this, a clearer understanding of the material behavior of the aortic tissue along the course of the disease is crucial. In this direction, Niestrawska et al. [9] proposed a three-stage biomechanical theory of AAA progression, in which aneurysm development is associated with intense G&R of the collagen fiber network. In short, stage 1 involves passive remodeling of the collagen fibers to the circumferential direction. This change is probably perceived by mechanotransduction mechanisms; hence cells react accordingly and remodel the collagen network, which leads to an increased compliance and the formation of a neo-adventitia on the abluminal side, which characterizes stage 2. As the disease progresses, this remodeling increases with considerable tissue stiffening and the build-up of the neo-adventitia (stage 3), which is characterized by a high degree of in-plane collagen isotropy.

The present work examines this newly developed mechanopathogenic model using FE simulations. For this purpose, the mechanical and histological constitutive parameters presented by Niestrawska et al. [9] are used for each stage to simulate four AAAs. The aim is to evaluate how the mechanical wall stresses change in the course of the disease and thus to shed light on biomechanical phenomena that are involved in the AAA pathogenesis.

Methods

Since Niestrawska et al. [9] found no correlation between aneurysm size and disease stage, 4 different AAA geometries, with diameters from 40 to 70mm, were examined. For each geometry, circumferential and axial wall stresses were calculated for stages 1 to 3, which resulted in a total of 12 simulations that were carried out in Abaqus 2017.

Geometry: The shape of the aneurysm is assumed to be axisymmetric (fusiform), described by the parametric equation [10, 11]

$$\mathrm{R(Z)} = \mathrm{R_a} + \left(\mathrm{R_{an}} - \mathrm{R_a} - \mathrm{c_3}\frac{\mathrm{Z}^2}{\mathrm{R_a}}\right)\exp\left(-\mathrm{c_2}\left|\frac{\mathrm{Z}}{\mathrm{R_a}}\right|^{\mathrm{c_1}}\right), \tag{1}$$

where $\mathrm{R(Z)}$ is the radius of the aneurysm in relation to the axial position Z, $\mathrm{R_{an}}$ denotes the maximum radius of the aneurysm, located at $\mathrm{Z} = 0$, and $\mathrm{R_a}$ represents the radius of the non-aneurysmatic region, taken as 15mm [1, 2]. The parameter c_1 is set to 5 and the geometric parameters c_2 and c_3 are given by Eqs. (2) and (3) [12], i.e.

$$\mathrm{c_2} = \frac{4.605}{(0.5\,\mathrm{L_{an}}/\mathrm{R_a})^{\mathrm{c_1}}}, \tag{2}$$

$$\mathrm{c_3} = \frac{\mathrm{R_{an}} - \mathrm{R_a}}{\mathrm{R_a}(0.8\,\mathrm{L_{an}}/\mathrm{R_a})^2}. \tag{3}$$

The ratio $\mathrm{F_L} = \mathrm{L_{an}}/\mathrm{R_{an}}$ has a value of 2.8 and determines the length of the aneurysmatic part L_{an} [13]. The length of the non-aneurysmatic part is chosen

Published by Verlag der TU Graz
Graz University of Technology

DOI: 10.3217/978-3-85125-826-4-07

to be 30% of L_{an}. Table 1 gives an overview of the values described above for the four AAA geometries.

Table 1: Overview of geometric parameters.

AAA radius R_{an} (mm)	AAA length L_{an} (mm)	Healthy length (mm)	Total length (mm)
20	56	16.8	98.6
25	70	21.0	112.0
30	84	25.2	134.4
35	98	29.4	156.8

The wall is modeled with a constant thickness of 1.5mm, which is a reasonable assumption for non-patient-specific geometries [12].

Material: The constitutive model of Gasser-Ogden-Holzapfel (GOH) [14] was used to characterize the material behavior of the AAA. It describes the tissue as an anisotropic hyperelastic material with a transversely isotropic fiber dispersion. While experimental evidence [15, 16] suggests that the amount of collagen dispersion in the circumferential-axial plane is usually higher than out-of-plane, the transversely isotropic GOH model has been used for simplicity, as it is readily available in Abaqus.

Niestrawska et al. [9] identified constitutive parameters for stages 1 to 3 by fitting the non-rotationally symmetric fiber dispersion model by Holzapfel et al. [15] to mechanical and histological data. In order to use these parameters with the GOH model, the transversely isotropic dispersion parameter was calculated by the relationship $\kappa = 1 - 2\kappa_{op}$ [13], where κ_{op} describes the out-of-plane dispersion [9]. The mean fiber angle α and the mechanical parameters c, k_1 and k_2, were taken directly from [9]. Table 2 summarizes the constitutive GOH parameters [14] for the three disease stages.

Table 2: Overview of constitutive parameters [9].

		Stage 1	Stage 2	Stage 3
c	[kPa]	0.95	1.83	3.78
k_1	[kPa]	1.30	0.46	8.96
k_2	[-]	98.6	112.0	156.8
κ	[-]	0.134	0.090	0.196
α	[°]	6.55	33.11	22.90

Mesh: Because of the axisymmetric nature of the problem, only one eighth of the aneurysm was modeled. For all four AAA geometries, the mesh consists of approximately 1100 C3D8H hybrid elements to take into account the assumption of incompressible behavior; the element size was selected after mesh convergence analyses (not shown here). Since there is no information about how the material parameters change in the radial direction, the mesh thickness consisted of a single element.

Boundary conditions: The displacements of the circumferential surfaces and the lower outlet surface were restricted according to (axi)symmetry. To the best of the authors' knowledge, there are no experimental data on pre-stretches in AAAs. In this study, an axial pre-stretching of 7% was applied to the upper outlet surface – a reasonable (healthy) value for an average patient age of 71 years [17] – while there was no pre-stretching in the circumferential direction. Finally, a pressure of 16kPa (120mmHg) was applied to the luminal surface, which resembled a (non-hypertensive) blood pressure load.

Results

Figure 1 shows the distribution of the circumferential Cauchy stresses σ_{circ} for all four AAA sizes and three disease stages. The simulation of the 70mm aneurysm did not converge for stage 1; however, we point out that such a large aneurysm is most likely not at the beginning of the disease and, therefore, the lack of this result should not affect the analysis.

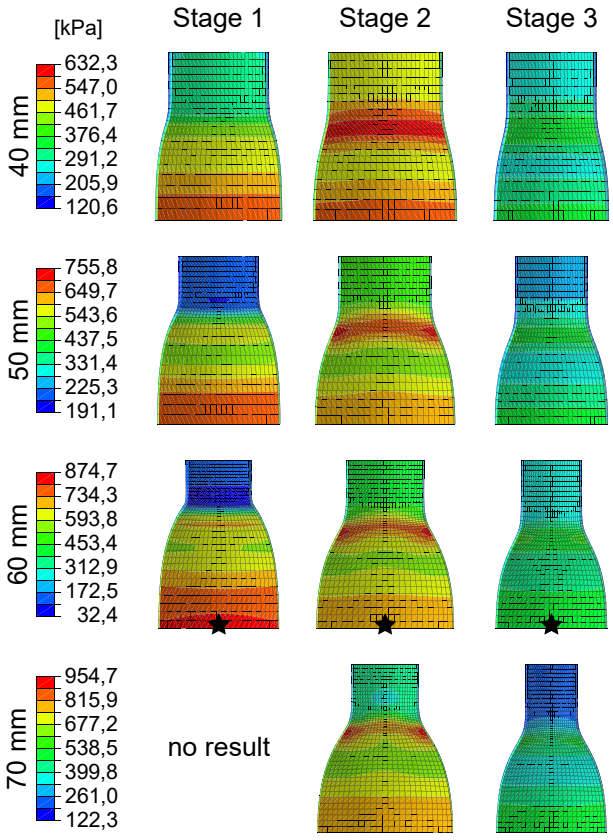

Figure 1: Distribution of the circumferential stress σ_{circ} on the luminal side of AAAs. Black stars identify the points used for plotting the stress-stretch curves of Fig. 4.

In Fig. 1, the maximum circumferential stress is always on the luminal side. In addition, the evolution of the circumferential stresses as the disease progression is similar for all aneurysm sizes: in stage 1 the maximum circumferential stress is in the sac (i.e. in the area of the maximum diameter); in stage 2 the stress value in the sac decreases slightly, but the maximum stress is now located in the neck area. In stage 3, the stresses decrease in

Published by Verlag der TU Graz
Graz University of Technology

DOI: 10.3217/978-3-85125-826-4-07

the entire domain, but the peak stress is still in the neck region.

Figure 2 shows the distribution of the axial Cauchy stresses σ_{axial} for all simulations. The maximum axial stress for all disease stages and all aneurysm sizes is always on the abluminal side of the sac. In general, the results of Figs. 1 and 2 agree well with earlier AAA simulations from the literature [12, 13], as well as with more recent *in vivo* measurements that identified, e.g., higher circumferential peak strain values on the neck of AAAs compared to the sac [18].

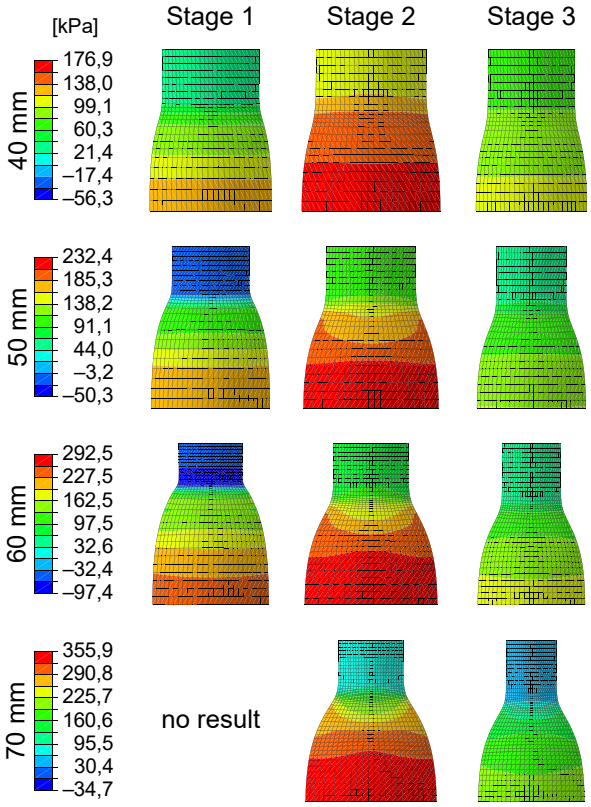

Figure 2: Distribution of the axial stress σ_{axial} on the abluminal side of the AAAs.

The maximum values of the stresses σ_{circ} and σ_{axial} for all simulations in Figs. 1 and 2 are summarized in Fig. 3, whereby it can be seen that the larger the aneurysm, the higher the stress values (in both directions), as expected. With regard to the development of the disease, the maximum stress values increase slightly from stage 1 to stage 2 (circumferential stress also changes location, see Fig. 1), while from stage 2 to stage 3 the maximum stresses in both directions decrease, which leads to stress values lower than stage 1. Interestingly, the percentage increase in the maximum circumferential stress (for the same stage) decreases with increasing size: for stage 2, e.g., the difference in maximum stress between the 40 and 50 mm AAAs is about 20%, while this increase is less than 10% between the 60 and 70mm AAAs. Although an idealized geometry is considered, this interesting result could in some way be related to the 5.5cm (empirical) threshold.

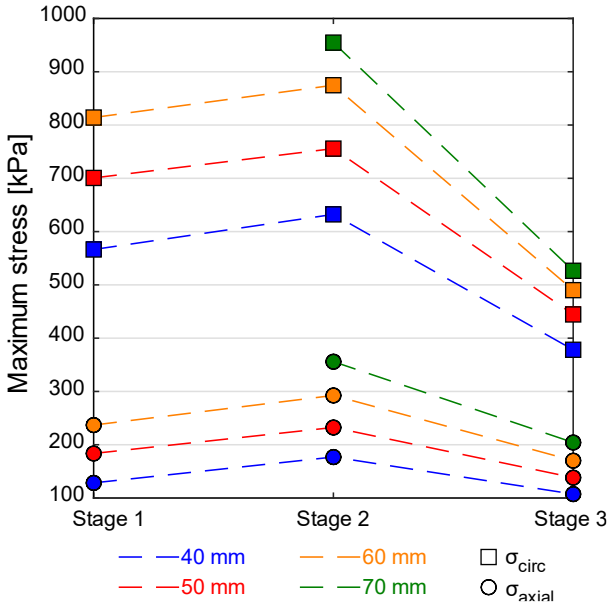

Figure 3: Maximum circumferential (squares) and axial stresses (circles) for different stages and aneurysm sizes.

Figure 4 shows circumferential stress-stretch curves for the three stages of the 60mm AAA, obtained from the same integration point located at the maximum AAA diameter (marked with black stars in Fig. 1). As expected, all curves are characterized by a linear slope (dominated by elastin) followed by a rapid increase in stress after collagen recruitment.

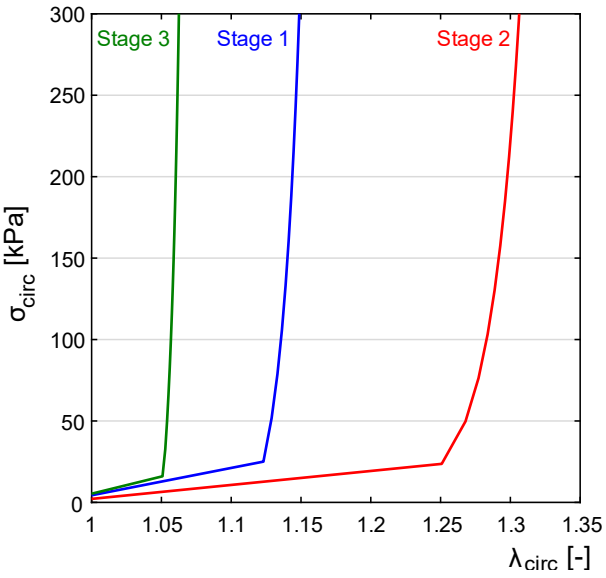

Figure 4: Circumferential stress-stretch curves for the three stages of the 60mm AAA.

The curves of Fig. 4 correspond to the definition of the disease stages by Niestrawska et al. [9], namely: the inflection point of stage 1 is between 1.1 and 1.15; stage 2 shows a more compliant behavior with an inflection point at $\lambda \geq 1{,}15$; and stage 3 shows a stiff behavior with an inflection point at $\lambda < 1{,}1$. These changes in the material stiffness of the tissue are also visible in Figs. 1 and 2, where the (compliant) stage

Published by Verlag der TU Graz
Graz University of Technology

DOI: 10.3217/978-3-85125-826-4-07

2 leads to the largest AAA diameter after pressurization, while the (stiff) stage 3 results in the smallest diameter. While the curves for the other AAA sizes are not shown here, the same behavior was observed.

Discussion

The clinical history of aortic aneurysms can be traced back to early descriptions by Roman and Greek doctors [19]; however, the pathogenesis of the disease has not yet been fully elucidated and decision-making criteria for assessing the risk of rupture are still predominantly empirical, based on diameter size [6, 7]. In this context, computer models such as the one presented here could contribute to a better understanding of the disease.

Numerical simulations of AAAs are not uncommon [12, 13]; in the present work, however, we have combined FE models with a more recent mechanopathogenic theory of development of aortic aneurysms, which was proposed by Niestrawska et al. [9]. Briefly, the authors identified three stages of the disease in which aneurysm development is associated with intense G&R of the collagen fiber network. It is believed that this G&R process consists of a reaction of mechanosensing vascular cells – particularly smooth muscle cells and fibroblasts – to (bio)mechanical changes related to the AAA pathogenesis in order to adapt the wall to the new configuration.

The results presented in Figs. 1 to 4 seem to support this hypothesis. First, by comparing stresses from the same column in Figs. 1 and 2, it can be seen that stopping the collagen remodeling process leads to increasing wall stresses, which, as expected, indicates an increasing risk of rupture in connection with aneurysm growth.

In the course of stage 1, on the abluminal side of the wall, Niewstrawska et al. [9] identified a passive reorientation of the mean fiber angle from the axial direction – characteristic of the healthy adventitia – to the circumferential direction, which is probably sensed by mechanotransducting cells (e.g., fibroblasts), which react accordingly and remodel the collagen network.

The associated changes (stage 2) lead to a slight decrease in the circumferential stresses on the aneurysm sac (Fig. 1), which is more pronounced in larger aneurysms. However, in this stage, axial stresses (Fig. 2) increase as well as the maximum circumferential stresses (Fig. 1), whose position is shifted from the sac to the AAA neck area. As the tissue also becomes more compliant (Fig. 4), greater dilatation due to blood pressure is clearly visible (Figs. 1, 2) and is likely to be perceived by the vascular cells.

Since the smooth muscle cells have largely disappeared at this stage [9], the further remodeling of the collagen network is promoted by fibroblasts, which increases the isotropy on the abluminal side of the wall (stage 3) [9]. Given the fusiform shape of most AAAs, it is worth noting that the shift towards a more isotropic (in-plane) fiber dispersion makes sense from a mechanical point of view. As a result, a considerable reduction in the stresses in both directions can be seen (Fig. 3). The decrease is more pronounced in the circumferential direction, where the maximum stress drops about 42% compared to stage 2 and by about 36% compared to stage 1. This is a direct result of the lower deformation (Figs. 1, 2) of the AAA resulting from the higher stiffness of the tissue (Fig. 4).

Disease progression (horizontal direction in Figs. 1, 2) and aneurysm growth (vertical direction in Figs. 1, 2) are simultaneous processes. Hence, a natural course of the disease would likely involve both. In this context, it is interesting to evaluate different stages combined with different diameters. The example of the circumferential stress (Fig. 1) shows that the maximum value initially rises from 566kPa (40mm, stage 1) to 756kPa (50mm, stage 2), but then drops to 490kPa (60mm, stage 3), i.e., below the initial value, which in turn suggests that collagen G&R could take place in an attemp to restore homeostasis.

It must be said, however, that these values are still much higher than those estimated for the healthy wall (~150kPa for the circumferential direction [13]), suggesting that if a healing process was actually in progress, either wall remodeling would persist or a new homeostatic state would have been established.

Conclusions and future work

There is a pressing need for better criteria for rupture risk assessment of AAAs that would enable the (bio)medical community to move forward from current empirical standards [8]. Using FE simulations to evaluate a recent three-stage theory for the development of AAAs [9], this study contributes to a better understanding of the pathogenesis of this disease.

The observed decrease in circumferential and axial stresses along disease progression (stages 1 to 3) appears to indicate an intentional healing process associated with collagen G&R promoted by vascular cells. As shown by Figs. 1 and 2, a lack of collagen remodeling leads to higher stresses during aneurysm growth, which indicates an increasing vulnerability of the vessel. Conversely, successful remodeling leads to significantly less stresses in the aortic wall (Fig. 3).

Future studies should use an appropriate non-rotationally symmetric fiber dispersion model [15] to validate these results, since arteries (both healthy and aneurysmatic) are known to be characterized by different amounts of in- and out-of-plane collagen fiber dispersion [16]. Furthermore, the effect of hypertension over the stability of the wall could be investigated by applying a pressure above 120 mmHg to the AAA.

Based on the histological state of the wall, Niestrawska et al. [9] identified two different stage 3 AAAs: vulnerable and potentially stable. Therefore, future work could also focus on differentiating these cases in order to gain better insights into a possible healing process in connection with the collagen remodeling.

Published by Verlag der TU Graz
Graz University of Technology

DOI: 10.3217/978-3-85125-826-4-07

References

[1] van der Vliet, J.A. and Boll, A.P.M.: Abdominal aortic aneurysm, *Lancet,* vol. 349, pp. 863-866, 1997.

[2] Sakahalisan, N., Limet, R. et al.: Abdominal aortic aneurysm, *Lancet,* vol. 365, pp. 1577-1589, 2005.

[3] Tillman, K., Lee, O.D. et al.: Abdominal aortic aneurysm: An often asymptomatic and fatal men's health issue, *Am. J. Men's Health,* vol. 7, pp. 163-168, 2013.

[4] Fleming, C., Whitlock, E.P. et al.: Screening for abdominal aortic aneurysm: A best-evidence systematic review for the U.S. Preventive Services Task Force, *Ann. Inter. Med.,* vol. 142, pp. 203-211, 2005.

[5] De Martino, R.R., Nolan, B.W. et al.: Outcomes of symptomatic abdominal aortic aneurysm repair, *J. Vasc. Surg.,* vol. 52, pp. 5-12, 2010.

[6] Brewster, D.C., Cronenwett, J.L. et al.: Guidelines for the treatment of abdominal aortic aneurysms: Report of a subcommittee of the Joint Council of the American Association for Vascular Surgery and Society for Vascular Surgery, *J. Vasc. Surg.,* vol. 37, pp. 1106-1117, 2003.

[7] Hirsch, A.T., Haskal, Z.J. et al.: ACC/AHA guidelines for the management of patients with peripheral arterial disease (lower extremity, renal, mesenteric, and abdominal aortic), *J. Vasc. Interv. Radiol.,* vol. 17, pp. 1383-1398, 2006.

[8] Vergaro, G., Del Corso, A. et al.: Biomarkers for growth prediction of abdominal aortic aneurysm: A step forward(?), *Eur. J. Prev. Cardiol.,* vol. 27, pp. 130-131, 2020.

[9] Niestrawska, J.A., Regitnig, P. et al.: The role of tissue remodeling in mechanics and pathogenesis of abdominal aortic aneurysms, *Acta Biomater.,* vol. 88, pp. 149-161, 2019.

[10] Elger, D.F., Blackketter, D.M. et al.: The influence of shape on the stresses in model abdominal aortic aneurysms, *J. Biomech. Eng.,* vol. 118, pp. 326-332, 1996.

[11] Roy, D., Holzapfel, G.A. et al.: Finite element analysis of abdominal aortic aneurysms: Geometrical and structural reconstruction with application of an anisotropic material model structural reconstruction with application of an anisotropic material model, *IMA J. Appl. Math.,* vol. 79, pp. 1011-1026, 2014.

[12] Rodríguez, J.F., Ruiz, C. et al.: Mechanical stresses in abdominal aortic aneurysms: Influence of diameter, asymmetry, and material anisotropy, *J. Biomech. Eng.,* vol. 130, p. 021023, 2008.

[13] Niestrawska, J.A., Haspinger, D.C. et al.: The influence of fiber dispersion on the mechanical response of aortic tissues in health and disease: a computational study, *Comput. Methods Biomech. Biomed. Engin.,* vol. 21, pp. 99-112, 2018.

[14] Gasser, T.C., Ogden, R.W. et al.: Hyperelastic modelling of arterial layers with distributed collagen fibre orientations, *J. R. Soc. Interface,* vol. 3, pp. 15-35, 2006.

[15] Holzapfel, G.A., Niestrawska, J.A. et al.: Modelling non-symmetric collagen fibre dispersion in arterial walls, *J. R. Soc. Interface,* vol. 12, p. 20150188, 2015.

[16] Niestrawska, J.A., Viertler, C. et al.: Microstructure and mechanics of healthy and aneurysmatic abdominal aortas: Experimental analysis and modelling, *J. R. Soc. Interface,* vol. 13, p. 20160620, 2016.

[17] Horny, L., Adamek, T. et al.: Analysis of axial prestretch in the abdominal aorta with reference to post mortem interval and degree of atherosclerosis, *J. Mech. Behav. Biomed. Mater.,* vol. 33, pp. 93-98, 2014.

[18] Derwich, W., Wittek, A. et al.: Comparison of abdominal aortic aneurysm sac and neck wall motion with 4D ultrasound imaging, *Eur. J. Vasc. Endovasc. Surg.,* vol. 60, pp. 539-547, 2020.

[19] S. G. Friedman, *A History of Vascular Surgery*, 2nd ed., Oxford: Blackwell Publishing, 2005.

Published by Verlag der TU Graz
Graz University of Technology